scientific reports

Check for updates

OPEN

Universality of ultrasonic attenuation coefficient of amorphous systems at low temperatures

Pragya Shukla

The competition between unretarded dispersion interactions between molecules prevailing at medium range order length scales and their phonon induced coupling at larger scales leads to appearance of nano-scale sub structures in amorphous systems. The complexity of intermolecular interactions gives rise to randomization of their operators. Based on a random matrix modelling of the Hamiltonian and its linear response to an external strain field, we show that the ultrasonic attenuation coefficient can be expressed as a ratio of two crucial length-scales related to molecular dynamics. A nearly constant value of the ratio for a wide range of materials then provides a theoretical explanation of the experimentally observed qualitative universality of the ultrasonic attenuation coefficient at low temperatures.

Experiments on thermal conductivity and acoustic attenuation in past have revealed an striking physical property of amorphous systems at low temperatures i.e. the universality of the internal friction Q^{-1}, defined in terms of the ratio of wavelength λ of the elastic wave to its mean free path l and a standard measure of the ultrasonic attenuation in the medium[1]. For $T = 0.1 \rightarrow 10$ K, $Q^{-1}(\omega; T)$ is found to be nearly independent of temperature T as well as measuring frequency ω. The magnitude of Q^{-1} not only lies within about a factor of 20 for all glasses but is also very small (around $\sim 10^{-4}$), indicating long (short) mean free paths at small (large) phonon frequencies.

Previous attempts to explain this behaviour were based on an assumed existence of the defects modeled as tunnelling two level systems (TTLS)[2]. Although successful in explaining many glass anomalies, the original TTLS model[3–6] suffered many drawbacks[7–9] (besides experimental lack of evidence supporting their existence in most glasses). This encouraged attempts for improvements of the model by incorporating a phonon-TTLS interaction[10], presence of TLS alongwith quasi-harmonic oscillators[11] as well as considerations of several new theories; (extensive research on this topic during previous decades renders it impossible to list all but a few leading to new theoretical developments e.g.[3–6,8,9,11–22]).

In context of the acoustic attenuation, an important direction was taken in a recent theory of coupled generic blocks with a phonon-mediated interaction of type $1/r^3$ with r as the separation between blocks[9,23]. A renormalisation approach used in Ref.[23] rendered the information regarding the behavior of a single generic block unnecessary and provided useful insights regarding the universality at macroscopic scales. Although the theory was later on applied successfully to explain another glass-universality, namely, Meissner–Berret ratio[24], it has still left many questions unanswered e.g. how the block type structure appears, what is the effect of the intra-block forces over the inter-block ones, whether the universality is an emergent phenomenon occurring only at large scales or it also occurs at microscopic scales i.e. for a single block; (for example, the study[23] does not provide any information about the attenuation coefficient for a basic block). An answer to these questions is pertinent to understand the physical origin of universalities which motivates the present work.

Based on the nature of chemical bonding, the physics of solids is expected to vary at microscopic length scales. Contrary to other low temperature properties, however the ratio λ/l is found to be universal not only for glasses (with only few exceptions in some thin films) but for a huge class of materials different from them at large length scales e.g. disordered crystals, poly-crystals, some quasi crystals etc[1]. Furthermore the irradiation experiments on crystalline silicon for a wide range of radiation doses indicate the sound properties of the irradiated samples similar to glasses. Another universality not confined only to glasses but applicable to many liquids too is that of excess vibrational density of states which can not be explained based on the phonon contributions only[25]. These universalities therefore seem to originate from more fundamental considerations, shared by both amorphous as

Department of Physics, Indian Institute of Technology, Kharagpur 721302, India. email: shukla@phy.iitkgp.ac.in

well as disordered crystalline materials, with lack of long-range order not the cause of the low-energy excitations, and applicable not only for macroscopic sizes but also at microscopic scales (e.g. see[26,27] also in this context). This motivated us in Ref.[28] to consider the intermolecular interactions, more specifically Vanderwaals (VW) forces among the molecules within a block as the basis for the behavior; it is important to emphasise here that VW forces among molecules are always present in all condensed phases and therefore are the natural candidates to decipher the experimentally observed universality.

Our primary focus in the present work is to seek the physical origin of the weak attenuation of the sound waves in amorphous systems. For this purpose, it is necessary to first identify the local structures which respond to an external strain field by collective vibrations of molecules. But phonons in a perfect harmonic dielectric crystal are free of interactions, leading to a sound wave travel unattenuated. To understand long mean free paths in glasses at low frequencies, this intuitively suggest to seek for ordered structure, at least locally, and repeated almost periodically. The structure related to medium range order (MRO) in glasses seem to be playing the relevant role. (Note the glasses also have short range order but that is governed by covalent bonds which are quite rigid to undergo deformation by a weak strain field. Further the role of the molecular clusters or structural correlations was proposed in past too e.g. in Refs.[25,29–31]) but it was not very well-defined[32]). As discussed in Ref.[33], the size of the basic block indeed turns out to be that of the length scale associated with medium range order (Note the peculiarity of role played by MRO in context of acoustic modes was mentioned in Ref.[32,34] too; the study[34] indicated that the continuum approximation for the medium, necessary for Debye formulation, breaks down for acoustic modes with wavelength less than MRO). The combination of many such blocks can then provide required periodicity and their long-range interaction result in attenuation only at long length scales. Our theory of coupled blocks is therefore based on two main types of interactions, dominant at different spatial scales; a competition between them governs the block-size and also gives rise to an inter-connected block structure, with phonon mediated coupling of their stress fields. This in turn leads to formulation of the attenuation in terms of the stress–stress correlations among basic blocks and their density of the states. As discussed later, both of them can be expressed in terms of the molecular properties which finally leads to a constant, system-independent average value of Q^{-1}.

The paper is organized as follows. The theory of an amorphous system of macroscopic size as a collection of sub-structures coupled with each other via an inverse-cube phonon mediated interaction is discussed in detail in Refs.[23,24]; this is briefly reviewed in "Super block: phonon mediated coupling of basic blocks" section, with macroscopic solid referred as the super block and the sub-structures referred as the basic blocks. Note the present work differs from Refs.[23,24] in context of the basic blocks details; the latter appear, in our theory, as a result of VW interactions among molecules prevailing at nano-scales[28]. The theory is used in "Ultrasonic attenuation coefficient: relation with stress matrix" section to relate the $\langle Q^{-1}\rangle$ of the super block to the stress-stress correlations of the basic blocks, their bulk density of states ρ_e and volume Ω_b; here $\langle\ \rangle$ refers to the ensemble as well as spectral average. ρ_e depends on a parameter b, referred as "bulk spectral parameter" and derived in Ref.[28] in terms of the molecular parameters. This along with Ω_b leads to dependence of Q^{-1} on the length-ratio R_0/R_v with R_0 as the linear size of the basic block and R_v as the distance between two nearest neighbor molecules mutually interacting by unretarded dispersion forces. A theoretical analysis of the ratio R_0/R_v has indicated it to be a system-independent constant for amorphous systems (supported by data based on 18 glasses)[33]. In "Qualitative universality of Q_a^{-1}" section, we express $\langle Q^{-1}\rangle$ in terms of R_0/R_v and thereby theoretically prove its quantitative universality. It can however be calculated directly from the molecular properties too; as discussed in "Comparison with experimental data" section, a good agreement of the results so obtained for 18 non-metallic glasses with experimental values not only lends credence to our theory of blocks but also provides an indirect route to reconfirm the universality of the ratio R_v/R_0. Note the 18 glasses chosen for comparison here are same as those used in Ref.[35]. A discussion of physical insights provided by our approach, brief comparison with other theories and approximations are outlined in "Discussion" section. We conclude in "Conclusion" section with a summary of our main ideas and results.

Super block: phonon mediated coupling of basic blocks

The order at atomic dimensions in an amorphous solid is system dependent; it is sensitive to the nature of chemical bonding. The intuition suggests the universal properties to originate from the interactions which appear at length scales at which the solid manifests no system-dependence. It is therefore relevant to seek and identify the sub-units in the super block structure which give rise to such interactions. For this purpose, let us first express the Hamiltonian H of the amorphous solid of volume Ω as the sum over intra-molecular interactions as well as inter-molecular ones

$$H = \sum_k h_k(\mathbf{r}_k) + \frac{1}{2}\sum_{k,l} \mathcal{U}(|\mathbf{r}_k - \mathbf{r}_l|), \tag{1}$$

with h_k as the Hamiltonian of the kth molecule at position $\mathbf{r}_k$ and $\mathcal{U}$ as an inter-molecular interaction with arbitrary range r_0. Assuming that all the relevant many body states are "localized", in the sense that the probability density for finding a given molecule "k" is "concentrated" (as defined by its mean square radius) in a region of finite radius l around some point $\mathbf{r}_k$, it is possible to define a $3D$ lattice (grid of points) $\mathbf{R}_\alpha$ with spacing $d \gg r_0$ such that the molecule "k" is associated with that lattice point $\mathbf{R}_\alpha$ which is closest to $\mathbf{R}_k$. The association is fixed, is insensitive to the dynamics and corresponds to representation of the solid by 3-dimensional blocks of linear size R_0, with their centers at lattice points $\mathbf{R}_\alpha$. The Hamiltonian H can then be reorganised as a sum over basic block Hamiltonians and the interactions between molecules on different blocks

$$H = \sum_s \mathcal{H}^{(s)} + \frac{1}{2}\sum_{s,t}\sum_{k\in s, l\in t} \mathcal{U}(|\mathbf{r}_k - \mathbf{r}_l|), \tag{2}$$

where $\mathcal{H}^{(s)}$ is the Hamiltonian of a basic block labeled "s", basically sum over the molecular interactions within the block: $\mathcal{H}^{(s)} = \sum_{k\in s} h_k(\mathbf{r}_k) + \frac{1}{2}\sum_{k,l\in s}\mathcal{U}(|\mathbf{r}_k - \mathbf{r}_l|)$. As mentioned below, the molecules interactions appearing in 2nd term in Eq. (2) rearrange themselves collectively and results in emergence of coupled stress fields of the blocks. The number g and volume Ω_b of these blocks can be determined by analysing the competition between inter-molecular forces with emerging forces i.e phonon mediated coupling: $g = \Omega/\Omega_b$ with $\Omega_b \sim R_0^3$. The statistical behavior of the Hamiltonian $\mathcal{H}$ is discussed in detail in Ref.[28].

To analyze the ultrasonic attenuation in glasses, we first need to analyze the response of $\mathcal{H}$ to an external strain field.

Perturbed Hamiltonian of a basic block. In presence of an external strain field, the molecules in a glass block are displaced from their equilibrium position and their interactions with those in surrounding blocks give rise to a stress field distributed over the block. Let $u(\mathbf{r})$ be the displacement, relative to some arbitrary reference frame, of the matter at point $\mathbf{r}$, the elastic strain tensor can then be defined as

$$e_{\alpha\beta}(\mathbf{r}, t) = \frac{1}{2}\left(\frac{\partial u_\alpha}{\partial x_\beta} + \frac{\partial u_\beta}{\partial x_\alpha}\right), \tag{3}$$

with subscripts α, β referring to the tensor-components.

This gives rise to stress in the block which can in general have both elastic as well as inelastic components. The perturbed Hamiltonian H_{pt} of the basic block, labeled "s" can then be written as a sum over elastic and inelastic contributions

$$\mathcal{H}^{(s)}_{pt} = \mathcal{H}^{(s)}_{pt,ph} + \mathcal{H}^{(s)}_{pt,nph}. \tag{4}$$

Each of these parts can further be expanded as a Taylor' series around unperturbed block Hamiltonian $\mathcal{H}_x$ in terms of strain $e_{\alpha\beta}$ in long wavelength limit (where the subscript "x" refers to the elastic ("$x = ph$") and inelastic parts ("$x = nph$") respectively):

$$\mathcal{H}^{(s)}_{pt,x}(t) = \mathcal{H}^{(s)}_x + \int \mathrm{d}\mathbf{r}\; e_{\alpha\beta}(\mathbf{r}, t)\; \Gamma^{(s)}_{\alpha\beta;x}(\mathbf{r}) + O(e^2_{\alpha\beta}), \tag{5}$$

with $\Gamma^{(s)}_{\alpha\beta;x}(\mathbf{r})$ as the stress tensor; as clear from above $\Gamma^{(s)}_{\alpha\beta;x}(\mathbf{r}) = \frac{\partial \mathcal{H}^{(s)}_{pt,x}}{\partial e_{\alpha\beta}}$. Here the retaintion of terms in the Taylor series expansion only up to first order in $e_{\alpha\beta}$ assumes the small strength of the strain field perturbation relatively to the unperturbed block Hamiltonian.

While a quantitative measure of the exact strength of the strain filed e.g. its weakness is not really needed for our analysis and is therefore beyond the purview of the present work, qualitatively the validity of Eq. (5) refers to a strength which permits (i) the treament of the block response to the external strain field within linear response theory (discussed in "Non-phonon linear response function" and in detail in Ref.[23]). We note the latter theory is used extensively for the mathematical formulation in this work, (ii) ignoring the rotation of the block etc under strain field, (iii) replacement of the distributed stress field within the block of volume Ω_b by an average field, acting from the centre of mass of the block: $\int_{\Omega_b} \mathrm{d}\mathbf{r}\; \Gamma^{(s)}_{\alpha\beta}(\mathbf{r}) = \Gamma^{(s)}_{\alpha\beta}$ (based on the assumption of the isotropy and the small block-size).

The perturbed Hamiltonian of the basic block can then be approximated as

$$\mathcal{H}^{(s)}_{pt;x} = \mathcal{H}^{(s)}_x + \sum_{\alpha\beta} e^{(s)}_{\alpha\beta}\; \Gamma^{(s)}_{\alpha\beta;x}, \tag{6}$$

with $e^{(s)}_{\alpha\beta}(t)$ referring to the phonon strain field $e_{\alpha\beta}(\mathbf{r}, t)$ at the s-th block.

Super block Hamiltonian. The super block consists of g basic blocks, perturbed by mutual interaction. To proceed further, it is useful to separate its Hamiltonian H into phononic and non-phonon contributions (referred by subscripts "ph" and "nph" respectively): $H = H_{ph} + H_{nph}$[9]. The contribution of elastic part H_{ph} to the ultrasonic attenuation in glass super block at temperatures $T < 1K$ is negligible. We therefore need to consider the contribution from the inelastic part H_{nph} only; to reduce notational complexity, henceforth, the subscripts "nph" will be suppressed and the notations $H, \mathcal{H}^{(s)}_{pt}, \Gamma^{(s)}$ etc will be used for $H_{nph}, \mathcal{H}^{(s)}_{pt;nph}, \Gamma^{(s)}_{nph}$ respectively.

As the strain tensor $e_{\alpha\beta}$ contains a contribution from the phonon field, the exchange of virtual phonons will give rise to an effective ("RKKY"-type) coupling between the stress tensors of any two block-pairs. Let $\Gamma^{(s)}_{\gamma\delta}(\mathbf{r})$ be the stress tensor at point $\mathbf{r}$ of the basic block "s". The interaction V_{st} between the blocks "s" and "t " can be given as[23]

$$V_{st} = \frac{1}{4\pi\rho_m c_t^2}\int_s \mathrm{d}\mathbf{r}\int_t \mathrm{d}\mathbf{r}'\sum_{te}\frac{\kappa^{(st)}_{\alpha\beta\gamma\delta}}{|\,\mathbf{r}-\mathbf{r}'\,|^3}.\;\Gamma^{(s)}_{\alpha\beta}(\mathbf{r})\otimes\;\Gamma^{(t)}_{\gamma\delta}(\mathbf{r}'), \tag{7}$$

with ρ_m as the mass-density and c_a, as the longitudinal (al) or transverse ($a \equiv t$) sound velocity in the super block. Here the subscripts $\alpha\beta\gamma\delta$ refer to the tensor components and the symbol $\sum_{te}$ refers to a sum over all tensor

components: $\sum_{te} \equiv \sum_{\alpha\beta\gamma\delta}$. The directional dependence of the interaction is represented by $\kappa^{(st)}_{\alpha\beta\gamma\delta} = \kappa^{(st)}(\theta,\phi)$; it is assumed to depend only on the relative orientation (θ,ϕ) of the block-pairs and is independent from their relative separation[24]:

$$\kappa^{(st)}_{ijkl} = -\left(\delta_{jl} - 3n_j n_l\right)\delta_{ik} + \nu_2 \Big[-(\delta_{ij}\delta_{kl} + \delta_{ik}\delta_{jl} + \delta_{il}\delta_{jk}) + \\ + 3\left(n_j n_l \delta_{ik} + n_j n_k \delta_{il} + n_i n_k \delta_{jl} + n_i n_l \delta_{jk} + n_i n_j \delta_{kl} + n_k n_l \delta_{ij}\right) - 15 \sum_{ijkl} n_i n_j n_k n_l \Big], \tag{8}$$

where $\nu_2 = \left(1 - \frac{c_t^2}{c_l^2}\right)$ and $\mathbf{n} = n_1\hat{i} + n_2\hat{j} + n_3\hat{k}$ is the unit vector along the direction of position vector $\mathbf{r} - \mathbf{r}'$. Again assuming the isotropy and the small block-size, the interaction between various points of the block-pairs can be replaced by the average interaction between their centers $\mathbf{R_s}$ and $\mathbf{R_t}$. The phonon mediate coupling between the blocks can then be approximated as[23,24]

$$V_{st} = \frac{1}{4\pi\rho_m c_t^2} \sum_{\alpha\beta\gamma\delta} \frac{\kappa^{(st)}_{\alpha\beta\gamma\delta}}{|\ \mathbf{R_s} - \mathbf{R_t}\ |^3}\ \Gamma^{(s)}_{\alpha\beta} \otimes\ \Gamma^{(t)}_{\gamma\delta}. \tag{9}$$

Due to the above emerging interactions at large length scales, the super block Hamiltonian in Eq. (2) is not just a sum over basic block Hamiltonians but also includes their phonon mediated coupling.

Equation (9) describes an emerging interaction at large length scales. The Hamiltonian of the super block in Eq. (2) can now be rearranged as a sum over those of the basic blocks as well as their phonon mediated coupling. In absence of external strain field, the non-phonon part of H can be rewritten as

$$H = H_0 + V, \tag{10}$$

with H_0 as a sum over non-phonon part of the unperturbed basic block Hamiltonians, $H_0 = \sum_{s=1}^{g}\ \mathcal{H}^{(s)}$, and, V as the net pair-wise interaction among blocks: $V = \sum_{s,t;s\neq t}\ V_{st}$ where $\sum_{s,t}$ implies the sum over all basic blocks. The presence of a weak external strain field perturbs the basic blocks and thereby H. The non-phonon part of the perturbed Hamiltonian H_{pt} can be written as[23,24]

$$H_{pt} = H + \sum_{s=1}^{g}\sum_{\alpha\beta} e^{(s)}_{\alpha\beta}\ \Gamma^{(s)}_{\alpha\beta} = H + \sum_{\alpha\beta} e_{\alpha\beta}\ \Gamma_{\alpha\beta}, \tag{11}$$

where the 2nd equality follows by assuming the same strain operator for all blocks $e^{(s)}_{\alpha\beta} \approx e_{\alpha\beta}$ and writing $\Gamma_{\alpha\beta} = \sum_{s=1}^{g}\Gamma^{(s)}_{\alpha\beta}$. (Note, as discussed in Ref.[24], the total Hamiltonian for the super block contains two additional terms besides V (see Eq. (2.21) in Ref.[24]) but their ensemble averaged contribution is negligible. Alternatively it can also be absorbed by redefining stress operators).

Ultrasonic attenuation coefficient: relation with stress matrix

In general, a wave propagating through a natural medium undergoes attenuation of its intensity with distance due to spreading, scattering as well absorption. For example, the change of amplitude in case of an attenuating plane wave can be expressed as $\Phi(x) = \Phi(0)\ e^{-\alpha x}$ with $\Phi(x)$ as the amplitude at position x and α as the "attenuation coefficient". The latter in general is a function of frequency ω, wave speed and quality factor of the medium and its measurement leads to the mean free path l of the wave $l = \alpha^{-1}$. For comparison of experiments on different materials, it is useful to a define the dimensionless ultrasonic attenuation coefficient $Q_a^{-1}(\omega)$ for a wave of frequency ν and wavelength λ[1,24]:

$$Q_a^{-1} = \frac{1}{2\pi^2}\frac{c_a}{\nu}\ \alpha = \frac{1}{2\pi^2}\ \frac{\lambda}{l}, \tag{12}$$

with c_a as the speed of acoustic wave in the longitudinal (with $a \equiv l$) or transverse direction ($a \equiv t$). Here we note that the above definition is different from the one given in Ref.[1] by a constant: $Q^{-1}_{a,pohl} = \pi\ Q_a^{-1}$. Further the quality factor of the medium corresponds to inverse of Q_a^{-1}; with former often defined as the "inverse internal friction", this in turn leads to Q_a^{-1} often referred as "intrenal friction" too.

Consider the attenuation of acoustic waves in a glass super block with its Hamiltonian H given by Eq. (11). Assuming the coupling between phonon and non-phonon degrees of freedom a weak perturbation on the phonon dynamics, $Q_a^{-1}(\omega)$ can be expressed as[24]

$$Q_a^{-1}(\omega) = (\pi\ \rho_m\ c_a^2)^{-1}\ \mathrm{Im}\ \chi_a(\omega), \tag{13}$$

with ρ_m as the mass-density of the material. Here $\chi_{l,t}(\omega)$, referred as the longitudinal or transverse response function, are the measures of the linear response of the basic blocks to external strain field and can be defined as follows; (see[23] for a detailed discussion).

Non-phonon linear response function. Consider the linear response of a basic block, labeled as "s", to an external strain field $e_{ij}(\mathbf{r},t) = e_{ij}\ exp[i(\mathbf{q}.\mathbf{r} - \omega t)]$ with e_{ij} real but infinitesimal. The perturbed Hamiltonian is given by Eq. (6) with corresponding stress-field given as $\Gamma^{(s)}_{ij}(\mathbf{r},t) = \hat{\Gamma}^{(s)}_{ij}\ exp[i(\mathbf{q}.\mathbf{r} - \omega t)]$ where $\langle\Gamma^{(s)}_{ij}\rangle$ is in general complex.

The complex response function or the susceptibility for a basic block can then be defined as

$$\chi^{(s)}_{\alpha\beta\gamma\delta}(\mathbf{q},\omega) \equiv \frac{1}{\Omega_b}\,\frac{\partial\,\hat{\Gamma}^{(s)}_{\alpha\beta}(\mathbf{q},\omega)}{\partial\,e_{\gamma\delta}}. \tag{14}$$

Here in general the variable $\mathbf{q}$ and ω are independent variables. But as our interest is in values of q close to $\omega/c_{l,t}$, χ will henceforth be written as a function of ω only[23].

The imaginary part of $\chi^{(s)}(\omega)$ can be written in the representation in which unperturbed basic block Hamiltonian $\mathcal{H}^{(s)}$ is diagonal (later referred as non-interacting or NI basis). Let $|m_s\rangle$, $m_s = 1 \to N$ be the many body eigenstate of $\mathcal{H}^{(s)}$ with energy e_m, then

$$\text{Im}\ \chi^{(s)}_{\alpha\beta\gamma\delta}(\omega) = \frac{(1-\mathrm{e}^{-\beta\omega})}{Z}\ \sum_m\ e^{-\beta e_m}\ \chi^{(m,s)}_{\alpha\beta;\gamma\delta}(\omega), \tag{15}$$

with Z as the partition function. Here to simplify presentation, we set $\hbar = 1$. Further

$$\chi^{(m,s)}_{\alpha\beta\gamma\delta}(\omega) = \frac{\pi}{\Omega_b}\ \sum_{n=1}^{N}\ \Gamma^{(s)}_{\alpha\beta;mn}\ \Gamma^{(s)}_{\gamma\delta;nm}\ \ \delta(e_n - e_m - \omega), \tag{16}$$

with $\Gamma^{(s)}_{\alpha\beta;kl}$ as the matrix element of the stress-tensor in the NI basis: $\Gamma^{(s)}_{\alpha\beta;kl} = \langle k_s|\ \Gamma^{(s)}_{\alpha\beta}\ |l_s\rangle$.

Substitution of Eqs. (15) and (16) in Eq. (13) leads to a frequency dependent formulation of Q_a^{-1} and thereby a dispersion of sound velocities (following from the Kramer–Kronig relations). However, as mentioned in "Introduction" section, extensive experimental studies during last few decades have clearly indicated a nearly temperature as well as frequency independence of the attenuation coefficient for a wide range of amorphous systems at low temperatures; these observations are also confirmed by independent measurements of dispersion in sound velocities in the medium[36]. Another rather more puzzling feature revealed by experiments is almost quantitative universality of Q^{-1} ($\approx 10^{-4}$) for many amorphous materials); these experimental findings are reviewed in detail in Ref.[1]. As such a small value of attenuation, equivalently long mean free paths of the phonons, in the amorphous medium is intuitively not obvious, this has baffled the researchers for last many decades (e.g. see[31]), has been an intense area of research and is also the primary focus of the present work. Hereafter, our present analysis would be confined to a frequency averaged ultrasonic attenuation coefficient only. While a detailed understanding of the qualitative universality i.e. frequency independence of Q^{-1} is also desirable, this requires a more detailed mathematical analysis of the stress–stress correlations and will be discussed in a subsequent work.

In general $\chi^{(m)}_{\alpha\beta\gamma\delta}$ depends on the energy level e_m and fluctuates over the spectrum. It is then useful to define the spectral averaged susceptibility over the N-level spectrum of the basic block

$$\langle\chi^{(s)}_{\alpha\beta\gamma\delta}\rangle_\omega = \frac{1}{N\omega_c}\sum_{m=1}^{N}\int_0^{\omega_c}\ \chi^{(m,s)}_{\alpha\beta\gamma\delta}(\omega - e_m)\ \mathrm{d}\omega, \tag{17}$$

where ω_c is the bulk spectrum width of the basic block with $\langle.\rangle_\omega$ implying a spectral averaging.

Furthermore the fluctuations of $\Gamma^{(s)}_{\alpha\beta;kl}$ as well as those of the energy levels over the ensemble also influence $\chi^{(m,s)}_{\alpha\beta\gamma\delta}(\omega)$ and it is appropriate to consider its ensemble average $\langle\chi^{(m,s)}_{\alpha\beta\gamma\delta}(\omega)\rangle_e$ too. Assuming isotropy, rotationally invariance of the basic block (as its linear size $L \gg a$ with a as the atomic length scale), all 3^8 components of response function can further be expressed in terms of the transverse and longitudinal response[24]:

$$\langle\chi^{(s)}_{\alpha\beta\gamma\delta}(\omega)\rangle_{e,\omega} = \left(q_c\ \delta_{\alpha\beta}\delta_{\gamma\delta} + \delta_{\alpha\gamma}\delta_{\beta\delta} + \delta_{\alpha\delta}\delta_{\beta\gamma}\right)\ \langle\chi^{(s)}_t\rangle_{e,\omega}, \tag{18}$$

where $q_c = \frac{\langle\chi^{(s)}_l\rangle_{e,\omega}}{\langle\chi^{(s)}_t\rangle_{e,\omega}} - 2$ along with $\langle.\rangle_e$ implying an ensemble averaging, $\langle.\rangle_{e,\omega}$ an averaging over both ω as well as ensemble.

The relations given in Eq. (14) to Eq. (18) are applicable for a basic block of volume ω_b. Following similar forms of Eqs. (6) and (11), these can be generalized for the susceptibility $\langle\chi_a\rangle^{sup}_{e,\omega}$ of a super block. This follows by dropping the superscript "s" and with replacements $\Omega_b \to \Omega$, $N \to N^g$, $\omega_c \to W_c$, $e_n \to E_n$ in Eq. (14) to Eq. (18); note here E_m refers to a many body energy level of H (defined in Eq. (10).

Relation between Q_a^{-1} and stress-correlations. *For basic block.* Due to disorder beyond atomic scales, a typical matrix element of the stress tensor of a basic block fluctuates over the ensemble and can be both positive as well as negative. This implies $\langle\Gamma^{(s)}_{\alpha\beta;kl}\rangle_e = 0$. Further, at temperature $T = 0$, the spectral averaging (defined in Eq. (17)) of Eq. (16) followed by an ensemble averaging leads to the stress-stress correlation of the basic block

$$\sum_{m,n=1}^{N}\langle\Gamma^{(s)}_{\alpha\beta;mn}\ \Gamma^{(s)}_{\gamma\delta;nm}\rangle_e = \frac{N\omega_c\ \Omega_b}{\pi}\left(q_c\ \delta_{\alpha\beta}\delta_{\gamma\delta} + \delta_{\alpha\gamma}\delta_{\beta\delta} + \delta_{\alpha\delta}\delta_{\beta\gamma}\right)\ \langle\text{Im}\ \chi^{(s)}_t\rangle_{e.\omega}, \tag{19}$$

where $\langle\text{Im}\ \chi^{(s)}_t\rangle_{e.\omega}$ is defined in Eq. (18).

The short-range order of atomic positions in the basic-block along with its small size suggests a homogeneous nature of many body interactions. The ensemble averaged matrix elements of $\Gamma^{(s)}_{\alpha\beta}$, in the NI basis i.e. the eigenfunction basis of $H^{(s)}_0$, can then be assumed to be of almost same strength. (This is equivalent

to say that, due to small size of block, stress can be assumed to be homogeneous i.e. of the same order everywhere in the block. This assumption therefore puts a constraint on our basic-block size). One can then write $\sum_{m,n=1}\langle\Gamma^{(s)}_{\alpha\beta;mn}\,\Gamma^{(s)}_{\gamma\delta;nm}\rangle_e = N^2\,\langle\Gamma^{(s)}_{\alpha\beta;mn}\,\Gamma^{(s)}_{\gamma\delta;nm}\rangle_e$. This on substitution in Eq. (19) leads to

$$\langle\Gamma^{(s)}_{\alpha\alpha;mn}\,\Gamma^{(s)}_{\gamma\gamma;mn}\rangle_e = \frac{\omega_c\,\Omega_b}{N\pi}\,\left[q_c+\delta_{\alpha\gamma}\right]\,\langle\mathrm{Im}\;\chi^{(s)}_t(\omega)\rangle_{e,\omega}, \tag{20}$$

$$\langle\Gamma^{(s)}_{\alpha\beta;mn}\,\Gamma^{(s)}_{\alpha\beta;mn}\rangle_e = \langle\Gamma^{(s)}_{\alpha\beta;mn}\,\Gamma^{(s)}_{\beta\alpha;mn}\rangle_e = \frac{\omega_c\,\Omega_b}{N\pi}\,\langle\mathrm{Im}\;\chi^{(s)}_t(\omega)\rangle_{e,\omega}\quad \alpha\neq\beta. \tag{21}$$

Further using Eq. (13) in Eqs. (20) and (21), the correlations can be expressed in terms of the average ultrasonic absorption $\langle Q_t^{-1}(\omega)\rangle_{e,\omega}$ of the basic block

$$\langle\Gamma^{(s)}_{\alpha\alpha;mn}\,\Gamma^{(s)}_{\gamma\gamma;mn}\rangle_e = N^{-1}\,\omega_c\,\rho_m\,c_t^2\,\Omega_b\,\langle Q_t^{-1}(\omega)\rangle_{e,\omega}\,\delta_{\alpha\gamma}, \tag{22}$$

$$\langle\Gamma^{(s)}_{\alpha\beta;mn}\,\Gamma^{(s)}_{\alpha\beta;mn}\rangle_e = \langle\Gamma^{(s)}_{\alpha\beta;mn}\,\Gamma^{(s)}_{\beta\alpha;mn}\rangle_e = N^{-1}\,\omega_c\,\rho_m\,c_a^2\,\Omega_b\langle Q_t^{-1}(\omega)\rangle_{e,\omega}. \tag{23}$$

Equation (23) can be rewritten in terms of the mean-square matrix element $v^2 = \langle\left(\Gamma^{(s)}_{\alpha\beta;mn}\right)^2\rangle_e$

$$\langle Q_a^{-1}\rangle_{e,\omega} = \frac{N\,v^2}{\omega_c\,\rho_m\,c_a^2\,\Omega_b} = \frac{\gamma^2}{\omega_c\,\rho_m\,c_a^2\,\Omega_b}, \tag{24}$$

where $\gamma^2 \equiv N^{-1}\,\mathrm{Tr}(\Gamma^{(s)}_{\alpha\beta})^2 = Nv^2$ is related to the coefficient of the phonon mediated coupling V between two basic blocks (which is of the form $\frac{\gamma^2}{8\pi\rho_m c^2 r^3}$, see Eq. (9)).

As discussed in Ref.[28], the ensemble averaged density of the states which participate in these excitations, has a universal form in the bulk of the spectrum: $\langle\rho_{bulk}(e)\rangle = \frac{Nb}{2\pi}\,\sqrt{2-(be)^2}$ with b later referred as the bulk spectral parameter and $\langle\;\rangle$ as the ensemble average; (note here $\langle\rho_e(e)\rangle$ is normalised to N: $\int\langle\rho_e(e)\rangle\;de = N$). This gives the bulk spectral width as

$$\omega_c = \frac{2\sqrt{2}}{b} = \frac{2N}{\pi\,\langle\rho_{bulk}(0)\rangle}. \tag{25}$$

As discussed in detail in Ref.[28], b can be expressed as

$$b \approx \frac{36}{\eta\,\sqrt{z\,g_0}\,A_H}\,\frac{y^6}{(1+y)^6} = \frac{9}{4\,\sqrt{3}\,A_H}\left(\frac{y}{1+y}\right)^{9/2}, \tag{26}$$

with A_H as the Hamaker constant of the material, z as the average number of nearest neighbors of a given molecule, g_0 as the number of molecules in the basic block, $\eta = \mathcal{N}-1$ with $\mathcal{N}$ as the number of relevant vibrational energy levels in a molecule). Based on the structural stability analysis of the amorphous systems, z is predicted to be of the order of 3 (for a three dimensional block)[4–6]. Further $\mathcal{N}$ corresponds to the number of single molecule states participating in dispersion interaction with another molecule. Alternatively, this is the number of dipole transitions among vibrational states of a molecule due to dispersion interaction with another one. Usually the allowed number of such transitions is 3 ($\delta m = 0,\pm1$ with m as the quantum number of the state); in any case weak nature of the dispersion interaction rules out higher number of such transitions).

For comparisons with TTLS model, it is worth noting that $\frac{1}{\omega_c\Omega_b}$ is of the order of the bulk-density per unit volume. This in turn renders $\langle Q_a^{-1}\rangle_{e,\omega}$ given by Eq. (24) analogous to that of TTLS model: $\langle Q_a^{-1}\rangle^{\mathrm{TTLS}}_{e,\omega} = \frac{\pi\,\gamma^2\,\overline{P}}{2\,\rho_m\,c_a^2}$ with $\overline{P}$ as the density of states of TTLS per unit volume.

For super block. Equation (24) corresponds to the average coefficient of attenuation in a basic block. Proceeding exactly as above, the average coefficient for a super block, say $\langle Q_a^{-1}\rangle^{sup}_{e,\omega}$, can also be obtained. The steps are as follows. Equation (19) is now replaced by the relation

$$\sum_{m,n=1}^{N^g}\langle\Gamma_{\alpha\beta;mn}\,\Gamma_{\gamma\delta;nm}\rangle_e = \frac{N^g\,W_c\,\Omega}{\pi}\left(q_c\,\delta_{\alpha\beta}\delta_{\gamma\delta}+\delta_{\alpha\gamma}\delta_{\beta\delta}+\delta_{\alpha\delta}\delta_{\beta\gamma}\right)\,\langle\mathrm{Im}\;\chi_t\rangle^{sup}_{e.\omega}, \tag{27}$$

where $\Gamma_{\alpha\beta;mn}$ refers to the matrix element of $\Gamma_{\alpha\beta}$ in the eigenbasis of H (Eq. (10)). But noting that the left side of Eq. (27) can be rewritten as $\langle\mathrm{Tr}(\Gamma_{\alpha\beta;mn})^2\rangle$ and is therefore basis-invariant, it can be evaluated in the eigenbasis of H_0 i.e the product basis of single block states referred as $|E_n^0\rangle, n = 1\rightarrow N^g$. Using

$$\Gamma_{\alpha\beta;mn} = \sum_{s=1}^{g}\Gamma^{(s)}_{\alpha\beta;mn}, \tag{28}$$

along with $\langle\Gamma^{(s)}_{\alpha\beta;mn}\Gamma^{t)}_{\alpha\beta;mn}\rangle = 0$, it is easy to see that

$$\sum_{m,n=1}^{N^g} \langle \Gamma_{\alpha\beta;mn}\, \Gamma_{\gamma\delta;nm} \rangle_e = g\, N^{g+1}\, \nu^2. \tag{29}$$

The above follows because $\Gamma^{(s)}_{\alpha\beta;mn} \neq 0$ only if the product states $|E^0_m\rangle$ and $|E^0_n\rangle$ differ only by the contribution from the s^{th} basic block. Further this also implies that the relevant spectral averaging for the super block is same as that of a basic block i.e $W_c = w_c$. The above, along with the definition $\langle Q_a^{-1} \rangle^{sup}_{e,\omega} = (\pi\ \rho_m\ c_a^2)^{-1}\ \langle \text{Im}\ \chi_a \rangle^{sup}_{e.\omega}$ and $\Omega = g\ \Omega_b$, now leads to

$$\langle Q_a^{-1} \rangle^{sup}_{e,\omega} = \frac{N\ g\ \nu^2}{\omega_c\ \rho_m\ c_a^2\ \Omega} = \frac{\gamma^2}{\omega_c\ \rho_m\ c_a^2\ \Omega_b}. \tag{30}$$

A comparison of the above result with Eq. (24) clearly indicates that

$$\langle Q_a^{-1} \rangle^{sup}_{e,\omega} = \langle Q_a^{-1} \rangle_{e,\omega}. \tag{31}$$

Qualitative universality of Q_a^{-1}

Based on unretarded dispersion interaction between molecules, Eq. (24) relates the ultrasonic attenuation coefficient $\langle Q_a^{-1} \rangle$ to the bulk spectrum width ω_c and thereby bulk spectrum parameter b. Equation (26) expresses b in terms of the molecular properties. Further as discussed in Ref.[33] in detail, the size t of the basic block can be expressed as

$$t^2 = \frac{R_0^3}{4\ R_v}. \tag{32}$$

Here R_v is the distance of closest separation between two molecules in the material and R_0 is a length scale at which the strength of dispersion interaction between two molecules (i.e. basic structural units[28]) is equal to the phonon mediated coupling of their stress fields[33]

$$R_0^3 = \frac{\rho_m\ c^2\ C_6}{8\gamma_m^2}, \tag{33}$$

with C_6 as the dispersion coefficient and γ_m as the coupling strength of the stress fields of the molecules. Using $\Omega_b = s\ t^3$, the above then gives the volume Ω_b of the basic block in terms of molecular parameters. Further, as discussed in Ref.[33], the number of molecules in a basic block can be given as

$$g_0 = \frac{\Omega_b}{\Omega_{\text{eff}}} \approx \frac{1}{(1+y)^3} \left(\frac{t}{R_m}\right)^3 = \frac{y^3}{8\ (1+y)^3} \left(\frac{R_0}{R_v}\right)^{9/2}, \tag{34}$$

with $y = \frac{R_v}{R_m}$ where R_m is the radius of the molecule.

A combination of the above relations then gives $\langle Q_a^{-1} \rangle$ in terms of the molecular properties. This can be derived as follows. A substitution of Eq. (26) in Eq. (24), along with above relations for t, R_0 and g_0 and $s = 4\pi/3$, leads to

$$\langle Q_a^{-1} \rangle_{e,\omega} \approx \frac{64\ \gamma^2}{2\ s\ \eta \sqrt{2 z g_0}\ \rho_m\ c^2\ C_6}\ \frac{R_v^6}{t_0^3}, \tag{35}$$

where, as discussed in Sect. I of SI files, γ, the coupling strength of basic blocks can be expressed in terms of that of molecules i.e γ_m,

$$\gamma^2 \approx \frac{4\ \pi\ g_0}{K\sqrt{2}}\ \gamma_m^2, \tag{36}$$

with

$$K^2 = 18\left(5 - 4\ \frac{c_t^2}{c_l^2}\right). \tag{37}$$

Using Eq. (33) to replace C_6 in the above equation leads to

$$\langle Q_a^{-1} \rangle_{e,\omega} \approx \frac{8\ \pi\ \sqrt{g_0}}{s\ \eta\ \sqrt{z}\ K}\ \frac{R_v^6}{R_0^3\ t^3}, \tag{38}$$

$$= \frac{32\ \pi}{s\ \eta\ \sqrt{2z}\ K} \left(\frac{y}{(1+y)}\right)^{3/2} \left(\frac{R_v}{R_0}\right)^{21/4}. \tag{39}$$

Here the 2nd equality is obtained by substitution of t and g_0 from Eqs. (32) and (34). Further, as mentioned below Eq. (26), $\eta = 2$ (with $\mathcal{N} = 3$ as the number of allowed dipole transitions in a molecule) and z as the number

of nearest neighbors of a molecule (those only interacting by VWD). The quantitative information about R_v available for a wide range of materials suggests $R_v \sim R_m$[37]. Taking $y = \frac{R_v}{R_m} \sim 1$ leads to, from Eq. (34), $g_0 \approx 8$. Assuming uniform mass density, this also implies only three nearest neighbor molecules to a given molecule within a spherical basic block of radius $t = \sqrt{\frac{R_0^3}{4\,R_v}}$ and therefore $z = 3$.

Following from Eq. (39), an almost quantitative universality of Q^{-1}, as experimentally predicted for amorphous systems[1], is not directly obvious. This however follows by noting that the length scales R_0 and R_v are related by a constant: $R_0 = 4R_v$[33]. Further the ratio $\frac{c_t}{c_l}$, and therefore K (from Eq. (37)), is known to be almost constant for many structural glasses[24,35]. Substitution of $\frac{R_0}{R_v} = 4$ in Eq. (39) along with $y \approx 1$ and $s = 4\pi/3$ leads to an almost material independent value of average internal friction

$$\langle Q_a^{-1}\rangle_{e,\omega} \approx 2.83 \times 10^{-4} \times \left(1.25 - \frac{c_t^2}{c_l^2}\right)^{-1/2}. \tag{40}$$

Previous experiments indicate that $\frac{c_l}{c_t}$ varies between $1.5 \rightarrow 2$, thus changing $\langle Q_a^{-1}\rangle_{e,\omega}$ within 10% only.

Further insight in the above result can be gained by rewriting $\langle Q_a^{-1}\rangle_{e,\omega}$ in terms of g_0, the number of molecules in a basic block. Substitution of Eq. (34) in Eq. (39) gives $\langle Q_a^{-1}\rangle_{e,\omega} \propto g_0^{-7/6}$. Further, using the relation $R_0 = 4R_v$ [33], Eq. (34) gives a constant, system-independent number of the molecules within each block: $g_0 = \frac{64\,y^3}{(1+y)^3}$. This in turn leads to a material independent value of the average ultrasonic attenuation coefficient $\langle Q^{-1}\rangle$. The above along with the definition given in Eq. (12) further suggests that the universality is brought about by the phonons of wavelength $\lambda \sim g_0\ l$ with l as their mean free path.

Taking typical value $R_m \sim 2.5{-}3.5$ Å gives $R_0 \sim 10{-}15$ Å which corresponds to the length scale for medium range topological order (MRO) (10 Å $\rightarrow$ 30 Å) (also see Table 3 of Ref.[33] for glass specific values of R_0) . This is as expected because VWD interactions are negligible beyond MRO and other interactions start dominating beyond this length scale.

Equation (40) is the central result of this paper. As described above, it is based on a balancing of the VW forces with phonon induced interactions among molecules at MRO length scales in amorphous systems. The universal aspects of this competition, as described above, then result in the qualitative universality of $\langle Q_a^{-1}\rangle_{e,\omega}$ which is consistent with experimental observations[1]. Note, based on the type of the experiment, the observed data for a glass often vary from one experiment to another (see for example, the values of tunnelling strengths $C_{l,t}$ in Ref.[1,35]).

Comparison with experimental data

Equations (39) and (40) both give theoretical formulations for the internal friction in terms of the molecular properties. Eq. (40) however is based on an additional prediction $R_0 = 4R_v$, derived and analyzed in Ref.[33]. This motivates us to compare both predictions, namely, Eqs. (39) and (40), with experimental data for 18 glasses given by two different studies[1] and[35].

A comparison of Eq. (40) with experiments requires the information only about c_l, c_t and is straightforward. But Eq. (39) depends on many other material properties and needs to be rewritten as follows. As discussed in Ref.[33], R_0 can be expressed in terms of molecular properties

$$R_0^3 = \frac{(1+y)^6\ c^2\ A_H\ M\ \Omega_m}{8\,\pi^2\,\gamma_m^2\,N_{av}}. = \frac{(1+y)^6\ \ A_H\ M^2\ c^2}{8\,\pi^2\,N_{av}^2\,\gamma_m^2\,\rho_m}. \tag{41}$$

Substitution of the relation $\Omega_m = \frac{4}{3}\pi\ R_m^3$ in Eq. (41) gives

$$\left(\frac{R_0}{R_v}\right)^3 = \frac{1}{y^3}\left(\frac{R_0}{R_m}\right)^3 = \frac{(1+y)^6}{y^3}\ \frac{M\ A_H}{6\ \pi\ N_{av}}\left(\frac{c}{\gamma_m}\right)^2. \tag{42}$$

Here c, as the speed of sound, and γ_m, as the phonon mediated coupling constant between molecules, have directional dependence: $c = c_l, c_t$ and $\gamma_m = \gamma_l, \gamma_t$ with subscripts l, t referring to longitudinal and transverse direction, respectively. The above along with Eq. (39) gives,

$$\langle Q_a^{-1}\rangle_{e,\omega} = \frac{48\,f(y)}{\eta\ \sqrt{2\ z}\ K}\left(\frac{6\ \pi\ N_{av}}{M\ A_H}\frac{\gamma_a^2}{c_a^2}\right)^{7/4}, \tag{43}$$

where $f(y) = \frac{y^{27/4}}{(1+y)^{12}}$ with $\eta = 2$, $z = 3$ and the subscript $a = l, t$. For later reference, note $f(y)$ is almost same for $y = 1$ and $y = 1.5$: $f(1) = 2.44 \times 10^{-4}$ and $f(1.5) = 2.59 \times 10^{-4}$.

As standard TTLS model is a special case of our generic block model, the available information for the coupling constants in the former case can be used for the latter (Note TTLS model is based on the presence of some two level atoms/molecules (TLS) as defects. The coupling constants of the molecules within a block due to molecule–phonon interaction can then be taken same as those of TLS). The TLS coupling constants are related to tunnelling strength C_a, defined as

$$C_a = \frac{\overline{P}}{\rho_m}\left(\frac{\gamma_a}{c_a}\right)^2, \tag{44}$$

Index		$\mathcal{B}_{l,bm}$	$C_{l,bm}$	$\mathcal{B}_{l,p1}$	$C_{l,p1}$	$\mathcal{B}_{l,p2}$	$C_{l,p2}$	$\mathcal{B}_{t,bm}$	$C_{t,bm}$	$\mathcal{B}_{t,p1}$	$C_{t,p1}$	$\mathcal{B}_{t,p2}$	$C_{t,p2}$	$\mathcal{B}_{th}$
Units	Glass	$\times 10^4$	$\times 10^4$	$\times 10^4$	$\times 10^4$	$\times 10^4$	$\times 10^4$	$\times 10^4$	$\times 10^4$	$\times 10^4$	$\times 10^4$	$\times 10^4$	$\times 10^4$	$\times 10^4$
1	a-SiO2	4.50	3.10	4.51	3.00	4.00	2.80	3.81	2.90	4.51	3.00	4.78	3.10	3.11
2	BK7	3.09	2.70					4.38	3.30					3.01
3	As2S3	0.76	1.60	1.64	2.30	0.69	1.40	1.48	2.00	0.96	1.70			2.88
4	LASF7	1.92	1.20	4.81	2.00			1.84	1.16					3.07
5	SF4	2.58	2.20					3.89	2.80					2.97
6	SF59	4.56	2.30					6.38	2.80					2.95
7	V52	2.46	4.00	5.03	6.00			3.46	4.90	4.18	5.40			2.88
8	BALNA	1.82	3.80					2.71	4.80					2.87
9	LAT	2.29	3.80					2.15	3.70					2.96
10	a-Se	0.65	1.20	0.88	2.20			0.82	2.20	1.42	2.90			2.86
11	Se75Ge25								0.90					
12	Se60Ge40	1.86		1.83	1.30			0.14	0.30					2.99
13	LiCl:7H2O	3.44	7.20	3.29	7.00			7.67	11.36	6.14	10.0			2.82
14	Zn-Glass	2.09	3.00					2.79	3.60					2.82
15	PMMA	1.55	2.00	4.57	3.70	3.35	3.10	4.90	3.70	7.21	4.80	9.73	5.70	2.82
16	PS	2.44	3.60			11.13	8.30	4.79	5.00	16.52	10.40	9.99	7.80	2.87
17	PC	1.00	1.80	3.51	3.50			3.19	3.30	31.23	12.20	20.16	9.50	2.77
18	ET1000	2.06	2.80	5.96	5.00			Inf						2.52

Table 1. Comparison of theoretical and experimental values of internal friction for 18 glasses with $M = M_1$: Here the theoretcial result from Eq. (47) labelled as $\mathcal{B}_{a,xx}$, with $a \equiv l, t$ are displayed in odd numbered columns for $M = M_1$. The 2nd subscript xx refers to the particular experiment used to obtain required parameters in Eq. (47): $xx \equiv bm, p1, p2$ for data from[35], $xx \equiv p1$ for accoustic data from[1], $xx \equiv p2$ for flexural data from[1]). The values used for M_1, c_l, c_t to obtain $\mathcal{B}_{a,xx}$ are given in Table 2, with experimental data for C_a given in adjacent even-numbered columns. The last column gives our theoretical prediction from Eq. (40).

with $\overline{P}$ as the spectral density of tunnelling states. According to tunnelling model,

$$C_a = \frac{2}{\pi}\,\langle Q^{-1}_{a,pohl}\rangle. \tag{45}$$

As the experimental results are usually given in terms of TTLS parameters C_l, C_t, we define the analog of C_a for our case for comparison

$$\mathcal{B}_a = \frac{2}{\pi}\,\langle Q^{-1}_{a,pohl}\rangle = 2\,\langle Q^{-1}_{a}\rangle. \tag{46}$$

The above along with Eqs. (43) and (44) then gives

$$\mathcal{B}_a = \frac{6\,f(y)}{\eta\,\sqrt{z}\,K}\left(\frac{6\,\pi\,N_{av}}{M\,A_H}\frac{\rho_m\,C_a}{\overline{P}}\right)^{7/4}. \tag{47}$$

Determination of physical parameters. Both definitions in Eqs. (45) and (46) refer to same physical property, i.e., internal friction, thus implying $\mathcal{B}_a = C_a$. From Eq. (47), however, $\mathcal{B}_a$ depends on many other parameters besides C_a which vary from one glass to another. Although, not obvious a priori how the two can be equal, this is indeed necessary if our theoretical prediction in Eq. (47) is consistent with the experimental values for $\langle Q^{-1}_a\rangle$. To verify the equality, we pursue a detailed quantitative analysis of $\mathcal{B}_l, \mathcal{B}_t$ for 18 glass. The required values of c_l, c_t to determine K along with ρ_m and $\overline{P}$ are taken from[35]. The information about C_a, A_H and M for the purpose is obtained as follows.

(i) C_l, C_t: Using ultrasonic absorption data, the study[35] determines C_l, C_t as adjustable parameters for 18 glasses; these values are displayed in columns 4 and 10 of Table 1 (referred as $C_{l,bm}$ and $C_{t,bm}$). The corresponding results for $\mathcal{B}_{l,t}$, derived from Eq. (47), are displayed in columns 3 and 9 of Table 1 (with notations defined in Table captions). The C_l, C_t-values mentioned in Ref.[1] for some of the glasses are different from[35] (although c_l, c_t values are same in both studies) which then lead to, from Eq. (44), different values for γ_l, γ_t. Further note that the study[1] considers data from two different experimental approaches, namely, acoustic and flexural) and the results for C_l, C_t values vary from one experiment to another. This motivates us to compare Eq. (47) with two sets of data given in Ref.[1] too. The C_l, C_t values from[1] are displayed in Table 1 in columns 6, 8, 12, 14; the latter along with ρ_m and $\overline{P}$ (both given in Table 2) are used to obtain corresponding theoretical predictions for $\mathcal{B}_l, \mathcal{B}_t$, given in columns 5, 7, 11, 13.

Index	Glass	ρ_m $\times 10^3$ kg/m^3	c_l km/s	c_t km/s	γ_l ev	γ_t ev	$\overline{P}$ 10^{45}/J m^3	A_H $\times 10^{-20}$ J	M_1 g/mole	Vwd unit	M_2 g/mole
1	a-SiO2	2.20	5.80	3.80	1.04	0.65	0.8	6.31	120.09	$[Si(SiO_4]$	60.08
2	BK7	2.51	6.20	3.80	0.9	0.65	1.1	7.40	92.81	$[SiO_4]$	65.84
3	As2S3	3.20	2.70	1.46	0.26	0.17	2.0	19.07	32.10	$[S]$	246.03
4	LASF	5.79	5.64	3.60	1.46	0.92	0.4	12.65	167.95	$[LASF]$	221.30
5	SF4	4.78	3.78	2.24	0.72	0.48	1.1	8.40	136.17	$[Si_2O_5]$	116.78
6	SF59	6.26	3.32	1.92	0.77	0.49	1.0	14.05	92.81	$[SiO_4]$	158.34
7	V52	4.80	4.15	2.25	0.87	0.52	1.7	8.37	167.21	$[ZrF_4]$	182.28
8	BALNA	4.28	4.30	2.30	0.75	0.45	2.1	6.87	167.21	$[ZrF_4]$	140.79
9	LAT	5.25	4.78	2.80	1.13	0.65	1.4	9.16	205.21	$[ZrF_6]$	215.69
10	a-Se	4.30	2.00	1.05	0.25	0.14	2.0	18.23	78.96	$[Se]$	78.96
11	Se75Ge25	4.35	0.00	1.24		0.15	1.0	22.19	77.38	$[Se_3Ge_1]$	77.38
12	Se60Ge40	4.25	2.40*	1.44*		0.16	0.4	23.56	76.43	$[Se_3Ge_1]$	76.43
13	LiCl:7H2O	1.20	4.00	2.00*	0.62	0.39	1.4	4.75	131.32	$[Li(H_2O)Cl_3]$	168.50
14	Zn-Glass	4.24	4.60	2.30	0.70	0.38	2.2	7.71	103.41	$[ZnF_2]$	103.41
15	PMMA	1.18	3.15	1.57	0.39	0.27	0.6	6.10	102.78	$[PMMA]$	102.78
16	PS	1.05	2.80	1.50	0.20	0.13	2.8	6.03	27.00	$[CH-CH2]$	105.15
17	PC	1.20	2.97	1.37*	0.28	0.18	0.9	6.00	77.10	$[C_6H_5]$	252.24
18	ET1000	1.20	3.25		0.35	0.22	1.1	4.91	77.10	$[C_6H_5]$	77.10

Table 2. Physical parameters for 18 glasses. The table lists the available data for the physical parameters appearing in Eqs. (39), (43) and (47). The $\rho, c_l, c_t, \overline{P}$ data from[35] (or[1] if not available in Ref.[35]) is displayed in columns 3rd, 4th, 5th and 8th, respectively. The columns 6th and 7th give the γ_l and the γ_t values, taken from Ref.[35] except for few cases; for those marked by a star (*), the values are obtained either from[1] or from C_l, C_t values given in Ref.[35] along with Eq. (45). Although not used for our analysis, the γ values are included here for completeness). The A_H values given in columns 9th are taken from Ref.[28]. The molar mass values, referred as M_1 for the vwd unit along with its composition is given in columns 10th and 11th and the mass M_2 for formula unit (same as glass molecular weight) in column 12th respectively.

(ii) M: As Eq. (47) depends on $M^{7/4}$, a correct estimation of M is important too. Two options available to determine M are (i) mass of the basic structural unit which dominates the structure of the glass and participates in the dispersion interaction (later referred as vwd unit), or, (ii) the molecular mass of the glass (later referred as formula unit); (here, for example for SiO_2 glass, SiO_2 is the formula unit but dominant structural unit can be SiO_4 or $Si(SiO4)$). Clearly, with dispersion interaction as the basis of our analysis, it is reasonable to use the 1st option . To analyze the influence however we consider both options to calculate $\mathcal{B}_l, \mathcal{B}_t$. The details of dominant structural unit for each glass and its mass, referred as M_1, is discussed in Sect. II of SI files. The formula mass, labelled here as M_2, corresponds to weighted summation of the molar masses of each constituent of the glass: for the latter consisting of n components $X_k, k = 1 \to n$, with their molar mass as m_k and weight percentage as p_k, $M_2 = \sum_{k=1}^{n} p_k\ m_k$. The glass composition for the 18 glasses is given in Sect. II of SI files and their M_1, M_2 values are displayed in Table 2.

(iii) A_H: for materials in which spectral optical properties are not available, two refractive-index based approximation for A_H namely, standard Tabor–Winterton approximation (TWA) (appropriate for low refractive index materials, $n < 1.8$) and single oscillator approximation (SOA) (for higher indexes $n > 1.8$), provide useful estimates[38] . The A_H for 18 glasses listed in Table 2 are based on these approximations (with details given in Ref.[28]).

Quantitative analysis. As mentioned above, Eq. (40) for $\langle Q_a^{-1}\rangle$ is based on relation $R_0 = 4R_v$ but Eq. (47) is based only on Eq. (33); (note Eq. (47) follows from Eq. (43)). The present analysis therefore provides two pathways to theoretically determine $\langle Q_a^{-1}\rangle$, one based on constant ratio of two short range length scales and other on molecular properties. The first pathway requires the information about c_l, c_t only but the second one also requires a prior information about the tunnelling strength C_a. The reported experimental data for the latter however varies significantly from one experiment to another (as indicated by the data from Refs.[1,35] in even numbered columns of Tables 1, 3). This in turn leads to different values of $\mathcal{B}_a$ (from Eq. (47)); the latter are displayed in odd-numbered columns of Tables 1 and 3 (for M_1 and M_2 respectively). Note, as displayed in Table 2, M_1 and M_2 do not differ significantly for the glass-ceramics and, consequently, the predictions for $\mathcal{B}_a$ for the two cases are close. However, for single component glasses e.g. SiO2 or where one component dominates (e.g. in BK7), $\mathcal{B}_l, \mathcal{B}_t$ predictions based on M_1 are closer to experimental data (see Table 1). This in turn provides further credence to the relevance of VW forces in present context.

The values of $\mathcal{B}_{th} = 2\langle Q_a^{-1}\rangle$ from Eq. (40), along with corresponding experimental C_a data for each glass, is also illustrated in Fig. 1. The similar comparison based on Eq. (47) is displayed in Fig. 2 for $M = M_1$ and Fig. 3

Index		$\mathcal{B}_{l,bm}$	$C_{l,bm}$	$\mathcal{B}_{l,p1}$	$C_{l,p1}$	$\mathcal{B}_{l,p2}$	$C_{l,p2}$	$\mathcal{B}_{t1,bm}$	$C_{t,bm}$	$\mathcal{B}_{t,p1}$	$C_{t,p1}$	$\mathcal{B}_{t,p2}$	$C_{t,p2}$	$\mathcal{B}_{th}$
Units	Glass	$\times 10^4$	$\times 10^4$	$\times 10^4$	$\times 10^4$	$\times 10^4$	$\times 10^4$	$\times 10^4$	$\times 10^4$	$\times 10^4$	$\times 10^4$	$\times 10^4$	$\times 10^4$	$\times 10^4$
1	a-SiO2	15.11	3.10	15.17	3.00	13.44	2.80	12.81	2.90	15.17	3.00	16.06	3.10	3.11
2	BK7	5.64	2.70					8.00	3.30					3.01
3	As2S3	0.02	1.60	0.05	2.30	0.02	1.40	0.04	2.00	0.03	1.70			2.88
4	LASF7	1.19	1.20	2.97	2.00			1.14	1.16					3.07
5	SF4	3.37	2.20					5.09	2.80					2.97
6	SF59	1.79	2.30					2.50	2.80					2.95
7	V52	2.11	4.00	4.33	6.00			2.97	4.90	3.60	5.40			2.88
8	BALNA	2.45	3.80					3.67	4.80					2.87
9	LAT	2.10	3.80					1.97	3.70					2.96
10	a-Se	0.65	1.20	0.88	2.20			0.82	2.20	1.42	2.90			2.86
11	Se75Ge25								0.90					
12	Se60Ge40	1.86		1.83	1.30			0.14	0.30					2.99
13	LiCl:7H2O	2.22	7.20	2.13	7.00			4.96	11.36	3.97	10.0			2.82
14	Zn-Glass	1.35	3.00					1.80	3.60					2.77
15	PMMA	1.55	2.00	4.57	3.70	3.35	3.10	4.90	3.70	7.21	4.80	9.73	5.70.	2.82
16	PS	0.23	3.60			1.03	8.30	0.44	5.00	1.53	10.40	0.93	7.80	2.87
17	PC	0.13	1.80	0.44	3.50			0.40	3.30	3.92	12.20	2.53	9.50	2.77
18	ET1000	2.06	2.80	5.96	5.00									2.52

Table 3. Comparison of theoretical and experimental values of internal friction for 18 glasses with $M = M_2$: All other details here are same as in Table 1.

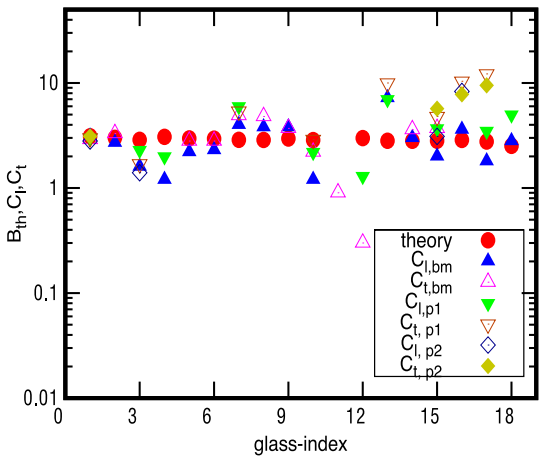

Figure 1. $\mathcal{B}_{th}$- values for 18 glasses: The figure depicts the theoretically predicted $\mathcal{B}_{th}$ from Eq. (40) and corresponding experimentally known tunneling strengths C_a with respect to glass-index (given in 1st column of Table 2). The symbol $C_{a,bm}$ refers to experimental data for tunneling strength from[35] and $C_{a,p1}$, $C_{a,p2}$ to acoustic and flexural data, respectively, from[1]. The values for B_{th} are also given in the last column of Tables 1 and 3; note these are same for both M_1, M_2.

for $M = M_2$. A direct comparison of theoretical and experimental data is also displayed in an alternative way in Fig. 4 for M_1 and in Fig. 5 for M_2. As mentioned above, the results for a glass vary from one experiment to other often within a factor of 2 but sometimes more e.g. for polymers (see odd numbered columns of Tables 1 and 3 and also[1]). But the deviation of our theoretical prediction from experiments is usually less than a factor of 2.

Further, a comparison of Figs. 2 and 3 (or Figs. 4, 5) indicates that the results for $M = M_1$ are closer to experimental data, thus indicating the molecules interacting by VWD interaction as an appropriate choice for the present analysis. This is also consistent with our theoretical approach assuming VWD interactions as the relevant interaction for length scales less than MRO.

An important point to note here is that the $\mathcal{B}_a$-dependence in Eq. (47) on glass-properties is based only on the product $M.A_H$. (This can be seen by substituting $R_0 = 4R_v$ in Eq. (41) which then gives the ratio $\frac{\gamma_m}{c}$ in terms of $M.A_H$ and thereby leads to an important result $\frac{\gamma_l}{\gamma_t} = \frac{c_l}{c_t}$[33]). The quantitative universality of $\langle Q^{-1} \rangle$ therefore seems to be a reconfirmation of already known relation between A_H and molar volume[39].

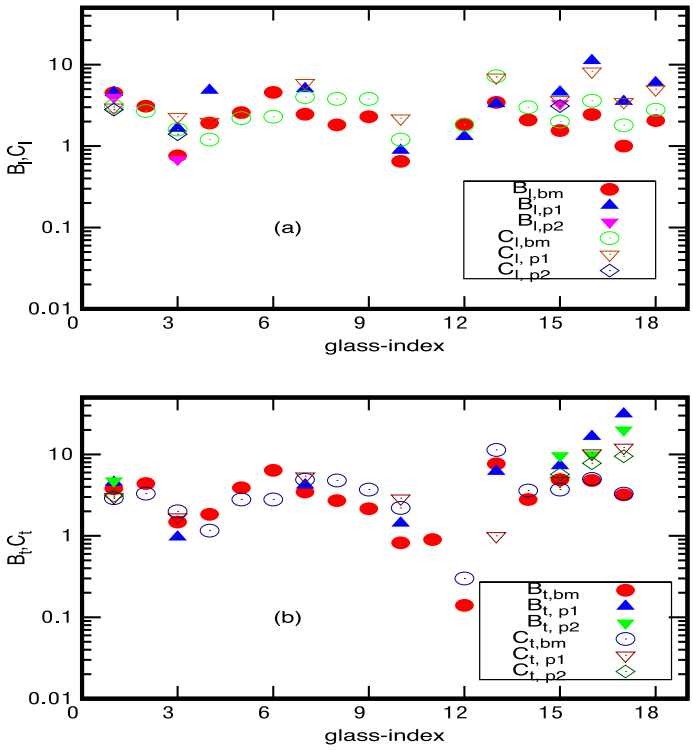

Figure 2. $\mathcal{B}_a$-values for 18 glasses (with $M = M_1$): The figure depicts the theoretically predicted $\mathcal{B}_a$ and corresponding experimentally known tunneling strengths C_a with respect to glass-index (all listed in Table 1). Here $\mathcal{B}_{a,xx}$ refers to Eq. (47) using tunneling parameters from different experiments (with $xx = bm$ referring to experimental data from[35], $xx = p1$ to acoustic and $xx = p2$ to flexural data from[1]). The symbols $C_{a,xx}$ refer to experimental data from[35] and[1] accordingly.

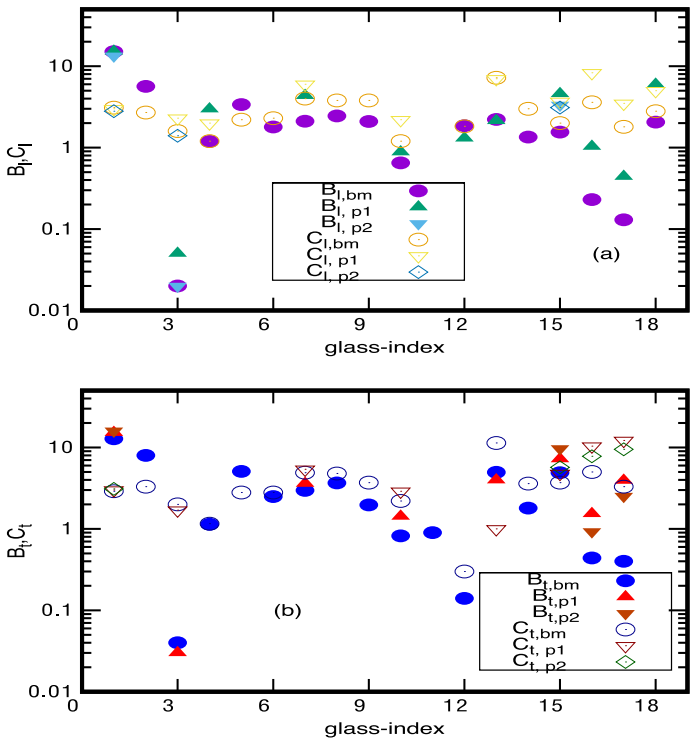

Figure 3. $\mathcal{B}_a$-values for 18 glasses (for $M = M_2$): All details are same as in Fig. 2 except that now the results for $\mathcal{B}_{a,xx}$ from Eq. (47) correspond to $M = M_2$. Note although the correspondence with experiments here is not as good as for M_1, the deviation however is still within a factor of 10. As reported in Ref.[1], the deviation of different experimental results lies also within that range.

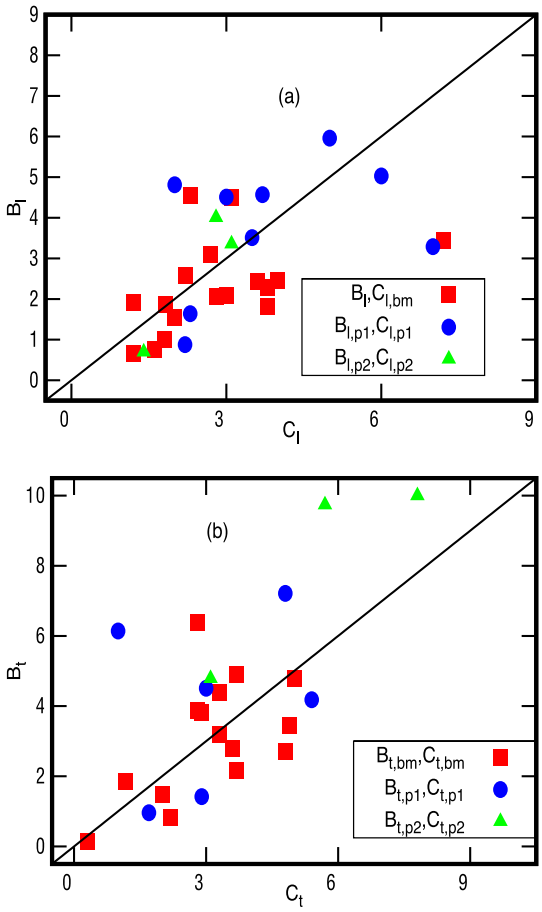

Figure 4. Comparison of $\mathcal{B}_a$-**values** ($a = l, t$), for 18 glasses from Eq. (47), for $M = M_1$, with their experimentally known tunneling strengths : here the $\mathcal{B}_{a1,xx}$-values correspond to y-coordinates of the points marked on the figure and $C_{a,xx}$ to their x-coordinates; the details of the labels are same as in Fig. 2. Here the solid line is shown only for visual guidance.

Discussion

The definition in Eq. (12), along with an almost constant Q_a^{-1}, implies a linear relation between the phonon mean free path l and its wavelength λ: $l \sim 10^3\lambda$. Within TTLS model, this behavior was explained by two different mechanisms: the low frequency phonons were postulated to be attenuated mainly by a relaxation of TLS defects but high frequency phonons that carry the heat were believed to be resonantly scattered[2,37]. Later on TLS were generalized to soft local atomic potentials (quasi-harmonic oscillators) and their interactions with phonons was attributed to be the cause of a constant Q^{-1}[11]. The approach however gave $C_a \sim 1$ i.e., a value three orders of magnitude too large; this later on led to suggestions that only a small fraction of the quasi-harmonic oscillators act as tunneling defects[11,40].

Although as discussed in Ref.[1], TTLS model shows good agreement for many glasses, the physical nature of tunnelling entities its not yet fully understood. Further the resemblance of the low-energy excitations in many disordered crystals to those found in amorphous solids strongly suggests their origin not related to long-range order in materials. It is therefore necessary to seek alternative theories especially those based on MRO i.e a length scale dominated by VW forces, present in all materials. This is indeed the case in our approach based only on two scales R_0 and R_v, the first of the order of MRO and second that of SRO. Note ideas suggesting a role of MRO scales in origin of glass anomalies have appeared in past too e.g.[29,25,32,34]. However these were based on experimentally/ numerically observed existence of structural correlations at these scales and did not explicitly consider the role of molecular interactions.

As Eq. (43) indicates, Q^{-1} depends only on the ratio $\frac{R_0}{R_v}$ which in turn is related to g_0, the number of molecules within the block. As the molecules interact by VW forces e.g by formation of induced dipoles that decay rapidly (i.e r^{-6}) with r as the distance between molecules, the dominant contribution comes from the nearest neighbor molecules only. Under acoustic perturbation, the molecules go to vibrational excited state by absorbing the energy from sound waves which triggers the induced dipole interactions among neighboring molecules. As this number can not vary much from one glass to another (assuming three dimensional structure) except for thin films, this results in a constant value of Q^{-1}. This also explains observed deviation in some thin films (see[1]). As indicated in Table 1, the value of Q^{-1} given by our approach for 18 glasses is in good agreement with experimental data.

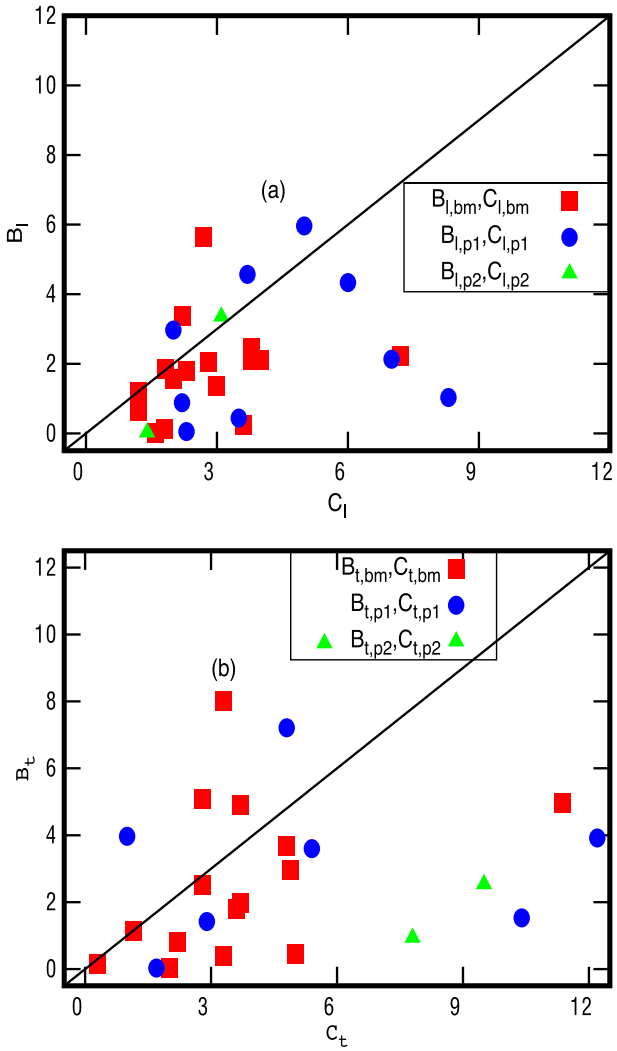

Figure 5. Comparison of $\mathcal{B}_a$-values ($a = l, t$), for 18 glasses from Eq. (47), for $M = M_2$, with their experimentally known tunneling strengths : here the $\mathcal{B}_{a1,xx}$-values correspond to y-coordinates of the points marked on the figure and $C_{a,xx}$ to their x-coordinates; the details of the labels are same as in Fig. 2. Here again the solid line is shown only for visual guidance.

Further physical insight in this consistency can be given as follows. As discussed in detail in Ref.[33], R_0 is also the size of the basic block and can be expressed in terms of molecular parameters. At large $\lambda > 2R_0$, the basic block subunits within a macroscopic glass block respond as an array of periodic structures which in turn ensures large mean free paths, thereby reducing the attenuation. For $\lambda \leq 2R_0$ however the orientational disorder of the induced dipoles at MRO scale or less affects the phonon dynamics causing their scattering and thereby localization. Thus R_0 is a relevant scale for the sound absorption and thereby attenuation in glasses; as discussed in Ref.[33], our R_0 is approximately the same as R of[32] (see Table 1 of Ref.[32]). The 2nd scale R_v appears in the wave-dynamics due to its sensitivity to the number of interacting molecules (from Eq. (34)). As the change of phonon dynamics occurs at length scale R_0, the Ioffe-Regel (IR) frequency ω_{ir} is therefore expected to correspond to $c_a/2R_0$, marking the transition from the well-defined acoustic like excitations to those characteristic of basic block, with $c_a = c_l, c_t$ as the sound velocity in the medium[33]. A comparison of our theoretical prediction $\omega_{ir} = c_a/2R_0$ with experimental available boson peak frequencies further indicates their closeness.

At this stage, it is worth reviewing the main assumptions made to arrive at our theoretical predictions:

(i) The interactions within the block are assumed to be homogeneous. The assumption was used in "Ultrasonic attenuation coefficient: relation with stress matrix" section for the random matrix modelling of the Hamiltonian as well as in linear response theory for Q^{-1}. This puts an upper limit on the allowed block size. As discussed in Ref.[33], the size of the block turns out to be of the medium range order $\sim$ 3 nm with only 8 molecules within, the assumption of homogeneity can be well satisfied.

Any block of bigger size would include both dispersion as well as phonon-coupling among molecules and thereby lead to inhomogeneity of the interactions. The theory in principle can still be adapted to

analyze a super block consisting of bigger basic block sizes (as in Ref.[23]) but it would need many modifications including the use of sparse random matrices. (Note with a radius R_0, the basic block considered here satisfies this condition).

(ii) The blocks are assumed to be of spherical shapes. This is a natural choice, keeping in view especially of the spherical shape of the molecules (although the latter is also an assumption but a standard one). It also helps a simpler technical formulation of the derivations. Alternatively, basic blocks of arbitrary shape can also be chosen but that is at the cost of technical complexity of intermediate steps of the derivation. We believe that although the ratio $\frac{R_0}{R_m}$ may vary slightly with shape but it will be compensated by the structure parameter s, thus leaving theoretical prediction in Eqs. (43) and (47) almost unaffected.

(iii) The interaction between phonon and non-phonon degrees of freedom are assumed to be weak, allowing linear response of the blocks to external perturbation.

The phonon mediated perturbation is assumed to access all N levels of the basic block Hamiltonian ($N = \mathcal{N}^g = 3^g$) within spectral range $\omega_c \sim 10^{-18}$ J (from Eq. (25). Although this gives the mean energy level spacing in the spectral bulk as $\Delta_b \approx \frac{\omega_c}{N}$ for a basic block is $\sim 10^{-22}$ J, the mean level spacing in the lower edge of the spectrum however is much smaller and levels can be accessed by thermal perturbation at low temperatures $T \sim 1$ K.

(iv) The dominant interactions at at MRO length scales of the glasses are non-retarded dispersion forces among molecules. This is applicable only to insulator glasses and needs to be replaced for other cases.

(v) The theoretical results presented here (Figs. 1, 2, 3, 4, Tables 1, 2, 3) are obtained from Eq. (47) with $y = R_v/R_m \sim 1$ for the molecules interacting by VWD. In general y fluctuates from one glass to another with 1 as its average value; the glass-specific values for y should be taken, in principle, for better accuracy. However as noted below Eq. (43), $f(y)$ remains almost same for $y = 1$ and $y = 1.5$: $f(1) = 2.44 \times 10^{-4}$ and $f(1.5) = 2.59 \times 10^{-4}$. The fluctuation of y therefore does not seem to have significant effect of our results.

(vi) The $\mathcal{B}_l, \mathcal{B}_t$ values given in Table 1 are obtained by approximate A_H values used in Eq. (43); we believe the results could be improved if exact values of A_H are used (see[39,38]). Further our results given in Table 1 are based on the Hamaker constant of the molecules interacting in vaccum. The vwd unit is however the dominant cation surrounded by other molecules; the interaction between two cations is therefore mediated by other molecules. It is natural to query, therefore, how the $\mathcal{B}_a$ results will be affected if A_H values in the relevant medium are considered.

Conclusion

In the end, we summarize with our main ideas and results.

Based on experimental evidence of ordered structure in glasses below MRO ($10 \rightarrow 30$ Å) and its lack above, we describe a macroscopic size glass material as elastically coupled, spherical shape, generic blocks, with homogeneous dispersion interaction within each such block. A random matrix modelling of their hamiltonian and linear response to an external strain field, then relates the low temperature averaged ultrasonic attenuation coefficient for the glass to a ratio of molecular length scales and a ratio of longitudinal and transverse sound speeds in the amorphous solid; the theoretical justification supported by numerical evidence for the former and experimental one for the latter indicate these ratios to be almost material independent. This in turn reveals the qualitative universality of the coefficient which is consistent with experimental observations in the temperature regime $1\ K \rightarrow 10\ \mathrm{K}$[1].

The central result of our work is given by Eqs. (39) and (40) with main assumptions summarised in "Conclusion" section. An important insight revealed by our formulation is the physical significance of the basic block size R_0: it is a length scale, typically of the order of MRO length scales in glasses, beyond which $\langle Q^{-1} \rangle$ attains universal value (As discussed in Ref.[33], R_0 is also the distance between two molecules at which two competing forces become equal in strength). Further R_0 is also consistent with another assumption made in our study i.e regarding the isotropy and homogeneity of the stress filed of the basic block; this follows because almost all molecules within a spherical block of radius R_0 are subjected to same interaction strength (with 8 molecules within a basic block). The omnipresence of dispersion forces indicates the application of our results to other disordered materials too.

The analysis presented here takes only dispersion type inter-molecular forces into account and neglects the induction forces which restricts, in principle, the application of our results to non-polar molecules. We believe however that inclusion of induction forces would only change numerical value of b (given by Eq. (26)) and would not affect the derivations given in "Super block: phonon mediated coupling of basic blocks" to "Discussion" sections. Similarly a generalization of the present theory by including electronic interactions may explain the universality in context of metallic glasses.

Received: 8 August 2021; Accepted: 1 February 2022
Published online: 17 February 2022

References

1. Pohl, R. O., Liu, X. & Thompson, E. Low-temperature thermal conductivity and acoustic attenuation in amorphous solids. *Rev. Mod. Phys.* **74**, 991 (2002).
2. Jackle, J. On the ultrasonic attenuation in glasses at low temperatures. *Z. Phys.* **257**, 212–223 (1972).
3. Anderson, P. W., Halperin, B. I. & Verma, C. M. Anomalous low-temperature thermal properties of glasses and spin glasses. *Philos. Mag.* **25**, 1–9 (1972).
4. Phillips, W. A. Two level states in glass, rep. *Prog. Phys.* **50**, 1657 (1987).

5. Brewer, D. F. (ed.) *Progress in Low-Temperature Physics* Vol. 9, 265 (Elsevier, 1986).
6. Jackle, J. *Amorphous Solids: Low-Temperature Properties* (Springer, 1981).
7. Galperin, Y. M., Karpov, V.G. & Solovjevv, N. 2. Eksp. Teor. Fiz. **94**, 373 (1988).
8. Leggett, A. J. & Yu, C. C. Low temperature properties of amorphous materials: Through a glass darkly. *Comments Condens. Matter Phys.* **14**, 231 (1988).
9. Leggett, A. J. & Vural, D. Tunneling two-level systems model of the low-temperature properties of glasses: Are smoking-gun tests possible? *J. Phys. Chem. B* **42**, 117 (2013).
10. Burin, A. L. & Kagan, Y. On the nature of the universal properties of amorphous solids. *Phys. Lett. A* **215**(3–4), 191 (1996).
11. Parashin, D. A. Interactions of soft atomic potentials and universality of low-temperature properties of glasses. *Phys. Rev. B* **49**, 9400 (1994).
12. Lubchenko, V. & Wolynes, P. G. Intrinsic quantum excitations of low temperature glasses. *Phys. Rev. Lett.* **87**, 195901 (2001).
13. Karpov, V. G., Klinger, M. I. & Ignatiev, F. N. Theory of the low-temperature anomalies in the thermal properties of amorphous structures. *Sov. Phys. JETP* **84**, 774 (1983).
14. Bucheanau, U. *et al.* Interaction of soft modes and sound waves in glasses. *Phys. Rev. B* **46**, 2798 (1992).
15. Schirmacher, W. Thermal conductivity of glassy materials and the boson peak. *Europhys. Lett.* **73**, 892 (2006).
16. Maruzzo, A., Schirmacher, W., Fratalocchi, A. & Ruocco, G. Heterogeneous shear elasticity of glasses: The origin of the boson peak. *Sci. Rep.* **3**, 1407 (2013).
17. Grigera, T., Martin-Mayor, V., Parisi, G. & Verrocchio, P. Phonon interpretation of the 'boson peak' in supercooled liquids. *Nature* **422**, 289 (2003).
18. Gurevich, V., Parashin, D. & Schrober, H. Anharmonicity, vibrational instability, and the Boson peak in glasses. *Phys. Rev. B* **67**, 094203 (2003).
19. Wyart, M. Scaling of phononic transport with connectivity in amorphous solids. *Euro. Phys. Lett.* **89**, 64001 (2010).
20. DeGiuli, E., Laversanne-Finot, A., During, G., Lerner, E. & Wyart, M. Effects of coordination and pressure on sound attenuation, boson peak and elasticity in amorphous solids. *Soft Matter* **10**, 5628 (2014).
21. Turlakov, M. Universal sound absorption in low-temperature amorphous solids. *Phys. Rev. Lett.* **93**, 035501 (2004).
22. Schechter, M. & stamp, P.C.E. Low temperature universality in disordered solids. http://arxiv.org/abs/09101283v1 (2009).
23. Vural, D. & Leggett, A. J. Universal sound absorption in amorphous solids: A theory of elastically coupled generic blocks. *J. Non Cryst. Solids* **357**, 3528 (2011).
24. Zhou, D. & Leggett, A. J. A generic microscopic theory for the universality of TTLS model Meissner–Berret ratio in low-temperature glasses. http://arxiv.org/abs/1510:05528v3.
25. Malinovsky, V. K., Novikov, V. N., Parashin, P. P., Solokov, A. P. & Zemlyanov, M. G. Universal form of the low-energy (2 to 10 meV) vibrational spectrum of glasses. *Europhys. Lett.* **11**, 43 (1990).
26. Chumakov, A. I. & Monaco, G. Understanding the atomic dynamics and thermodynamics of glasses: Status and outlook. *Non-Cryst. J. Solids* **407**, 126 (2015).
27. Chumakov, A. I. & Monaco, G. Relation between the boson peak in glasses and van Hove singularity in crystals. *Non-Cryst. Philos. Mag.* **96**, 1 (2015).
28. Shukla, P. Low temperature heat capacity of nanosize amorphous solids. *J. Phys. Condens. Matter* **33**, 455301. https://doi.org/10.1088/1361-648X/ac1cb3 (2021).
29. Duval, E., Boukenter, A. & Achibat, T. Vibrational dynamics and the structure of glasses. *J. Phys. Condens. Matter* **2**, 10227 (1990).
30. Graebner, J. E., Golding, B. & Allen, L. C. Phonon localization in glasses. *Phys. Rev. B* **34**, 5696 (1986).
31. Yu, C. C. & Freeman, J. J. Thermal conductivity and specific heat of glasses. *Phys. Rev. B* **36**, 7620 (1987).
32. Elliott, S. R. A unified model for the low-energy vibrational behaviour of amorphous solids. *Europhys. Lett.* **19**, 201 (1992).
33. Shukla, P. http://arxiv.org/abs/2101.00492.
34. Monaco, G. & Giordano, V. M. Breakdown of the Debye approximation for the acoustic modes with nanometric wavelengths in glasses. *PNAS* **106**, 3659 (2009).
35. Berret, J. F. & Meissner, M. How universal are the low temperature acoustic properties of glasses? *Z. Phys. B-Condens. Matter* **70**, 65 (1988).
36. Hucklinger, S. Phonons in amorphous materials. *J. Phys.* **43**, c9 (1982).
37. Phillips, J. C. Topology of covalent non-crystalline solids II: Medium-range order in chalcogenide alloys and A Si(Ge). *J. Non-Cryst. Solids* **43**, 37 (1981).
38. French, R. H. Origins and applications of London dispersion forces and Hamaker constants in ceramics. *J. Am. Ceram. Soc.* **83**, 2117 (2000).
39. Israelachvili, J. *Intermolecular and Surface Forces* 3rd edn. (Academic Press, 2011).
40. Parashin, D. A., Schrober, H. R. & Gurevich, V. L. Vibrational instability, two-level systems, and the boson peak in glasses. *Phys. Rev. B* **76**, 064206 (2007).

Acknowledgements

I am grateful to Professor Anthony Leggett for introducing me to this rich subject and intellectual support in form of many helpful critical comments and insights. The financial support provided by SERB, DST, India under Matrics grant scheme is also gratefully acknowledged.

Author contributions

The paper has a single author contributing to the manuscript.

Competing interests

The author declares no competing interests.

Additional information

Supplementary Information The online version contains supplementary material available at https://doi.org/10.1038/s41598-022-06589-7.

Correspondence and requests for materials should be addressed to P.S.

Reprints and permissions information is available at www.nature.com/reprints.

Publisher's note Springer Nature remains neutral with regard to jurisdictional claims in published maps and institutional affiliations.